

# A FINITE ELEMENT METHOD FOR THE SHALLOW WATER EQUATIONS

by

A. HAUGUEL (1), G. LABADIE (2) and B. LATTEUX (3)

## ABSTRACT

The paper reports the current progress in developing a finite element method for the shallow water equations. The main feature of the method is the special care given to the advective and diffusive parts of the equations, so that it can be of interest to use it when dealing with flows strongly influenced by convective and boundary layer effects. The solution procedure has been chosen so as to allow a calculation with a big number of nodes.

Section 3 of the paper outlines the method. In section 4, is detailed the procedure for the advective terms, involving the determination of the characteristic curves. Section 5 is devoted to the diffusion and propagation terms. Finally numerical results are presented in section 6.

## 1. INTRODUCTION

Environmental hydraulics often requires the calculation of flows in complex domains. Moreover, one often wishes a finer description for some zones of particular interest, while most of the domain can be approximated by a rather coarse grid. The finite element method provides such a flexibility and a growing interest is taken in its potential.

However the size of the resulting discrete system restricts the possibilities of using it. An interesting approach, presented here, leads to consider separate problems on each of the scalar variables (water level and flow discharge components) and hence allows to reduce the storage requirement.

- 
- (1) Head of the Research Hydraulic Division, Laboratoire National d'Hydraulique, E.D.F., Chatou, France.
  - (2) Research Engineer, Laboratoire National d'Hydraulique, E.D.F., Chatou, France.
  - (3) Research Engineer, Laboratoire National d'Hydraulique, E.D.F., Chatou, France.

## 2. NOTATION

$F$	= Coriolis and friction forces (components $F_i$ )
$\vec{g}$	= acceleration due to gravity
$h$	= depth of water
$h_m$	= average of $h$ in time
$K$	= momentum diffusion coefficient
$Q$	= $uh$ flow rate per unit length (components $Q_i$ )
$\vec{u}$	= velocity field (components $u_i$ )
$z$	= free surface elevation.

## 3. EQUATIONS

The shallow water equations consist of the mass conservation equation and two momentum equations :

$$\frac{\partial z}{\partial t} + \nabla \cdot \vec{Q} = 0$$

$$(1) \quad \frac{\partial Q_i}{\partial t} + \nabla \cdot (Q_i \vec{u}) + gh \frac{\partial z}{\partial x_i} - K \Delta Q_i = F_i$$

A fractional step algorithm is used to decompose the equations into a pure convection system and the remainder.

$Q^n$ ,  $Z^n$  being given at time  $t^n$ , the unknowns at time  $t^{n+1}$ ,  $Q^{n+1}$ ,  $Z^{n+1}$  are computed by the two following successive steps :

- Determination of auxiliary unknown  $Q^{n+\frac{1}{2}}$  solution of the convection equations :

$$(2) \quad \frac{\partial Q_i}{\partial t} + \nabla \cdot (Q_i \vec{u}^n) = 0$$

- Resolution of the diffusion and propagation problem :

$$\frac{\partial z}{\partial t} + \nabla \cdot \vec{Q} = 0$$

$$(3) \quad \frac{\partial Q_i}{\partial t} - K \Delta Q_i + gh \frac{\partial z}{\partial x_i} = F_i$$

with initial conditions  $Z^n$ ,  $Q^{n+\frac{1}{2}}$

#### 4. ADVECTION STEP

It involves the resolution of equations (2), which can be transformed into equations on velocity, by use of the continuity equation :

$$(4) \frac{\partial u_i}{\partial t} + u_i^n : \nabla u_i = 0$$

This form has been preferred to the original form (2) as explained in section 6.

A characteristics method has been used to solve those equations (4). It requires two steps :

- computation of the characteristic curves passing through the nodal points ;
- interpolation at the foot of those curves.

The method is unconditionally stable and the time step has just to be small enough to catch the time variation of the velocity field  $u_i$ .

Moreover the amount of computation needed is very reasonable. In particular, there is no non-symmetric system to assemble and solve at each time step, as would appear in a standard implicit method.

As for accuracy, it is quite satisfactory, although somewhat depending on the time-step : the only significant error being made when performing the interpolation at the foot  $P_j$  of the characteristic, the accuracy decreases when  $P_j$  is far from a mesh-point, particularly when using a linear interpolation. Finally, conservativity is not ensured by the scheme ; this is probably the main drawback of the method.

This technique has been applied for a long time in the solution of the Navier Stokes equations and is described in more detail in [1]. Some more research is done on the subject [2].

#### 5. DIFFUSION AND PROPAGATION STEP

An implicit discretization has been chosen for system (3) except for the non linear term  $ghVZ$  which is partly explicit. There is no need for a second order scheme in time for such long waves as the tide.

If we drop, for sake of simplicity, the superscripts  $n+1$ , the system to solve in this step is of the form :

$$(5) \alpha z + \nabla \cdot Q = R$$

$$(6) \alpha \underset{\sim}{Q} - K \Delta \underset{\sim}{Q} + g h_m \nabla z = \underset{\sim}{T}$$

with :  $\alpha = \frac{1}{DT}$  ;  $R = \frac{1}{DT} z^n$  , and  $\underset{\sim}{T} = \frac{1}{DT} \underset{\sim}{Q} + F^n - g(h^n - h_m) \nabla z^n$

( $h_m$  being the average in time of  $h$ , that is a function of space coordinates only).

The discretization of equations (5), (6) with their boundary conditions ( $Q$  given) yields to a large size linear system. A natural idea to reduce this size, is to eliminate  $Q$  between equations (5) and (6). This is achieved by applying the divergence operator to (6) and plugging (5) into the result. The equation obtained is :

$$(7) \alpha^2 z - \nabla \cdot (K \alpha + g h_m) \nabla z = W$$

with :  $W = \alpha R - K \Delta \underset{\sim}{R} - \nabla \cdot \underset{\sim}{T}$ .

Equation (7) is an elliptic equation, giving by discretization a symmetric matrix. It can easily be solved if a boundary condition is provided for  $z$ . If so,  $Q$  can be straight forwardly computed from equation (6) where the term  $g h_m \nabla z$  is now a known function and can be rejected into the right hand side. With Dirichlet boundary conditions, equation (6) decomposes into two decoupled equations, one for each component  $Q_i$  of  $Q$  leading to the same symmetric matrix for the discrete system.

The problem then amounts to the determination of the trace of  $z$  on the boundary. The procedure used for this purpose is an extension of the technique proposed by Glowinski-Pironneau [3] for the Stokes problem. It is described in detail in [5].

This technique is advantageous on the point of view of computational efficiency. Two "domain" matrices have to be stored, one for the variable  $z$ , another for each component of  $Q$  (it is the same matrix for the two components). They are symmetric and sparse and small enough to be processed by an in-core solver such as an incomplete Choleski preconditioned conjugate gradient. In addition, the matrix of the boundary operator has to be factorized and stored.

## 6. NUMERICAL RESULTS

Several applications have been performed, from a very schematic case, in order to have a first view on the possible problems, to a realistic complex one, to give a more comprehensive test of the method.

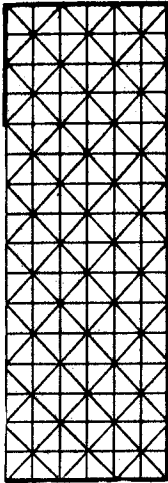


Fig.1. Finite elements discretization

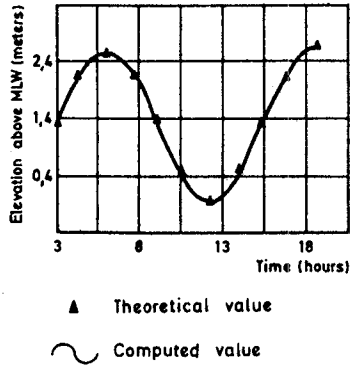
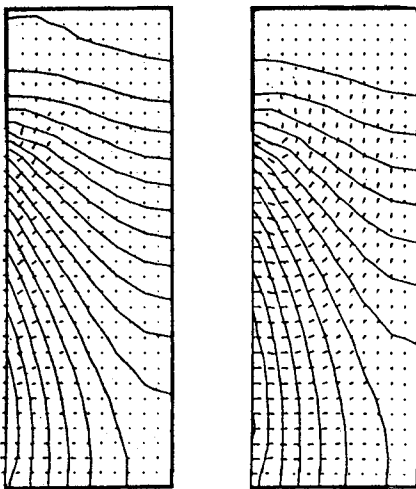


Fig.2. Average surface elevation



Low water

High water

Fig.3  
Velocity fields and  
free surface  
elevation lines

SCHMATIZED MASSACHUSSETS BAY

### 6.1. Schematized Massachussets Bay

In this first experiment, emphasis has been laid on the general behaviour of the method rather than the comparison with actual data. Thus neither the friction and Coriolis force, nor the varying bottom topography were simulated. The domain was coarsely approximated by a rectangle (fig.1) divided into 192 triangular elements with respectively 119 and 429 nodes for piecewise linear and quadratic approximations. Both components of the flow discharge were prescribed on the boundaries ; this discharge was taken to be zero on the land limits, and was schematized on the ocean limit by a sinusoidal uniform flow.

Results as regards current fields and free surface elevation (fig. 2 and 3) were found to be quite satisfactory ; in particular global mass conversation has been insured at less than 1% of the total mass flux over a whole tide.

Teachings of this first application are as follows :

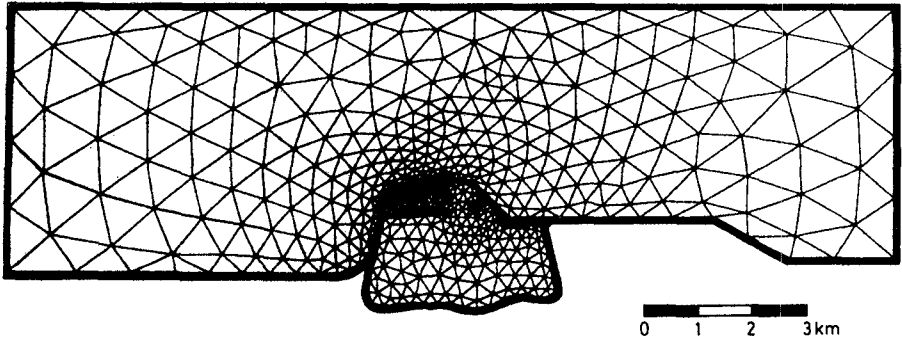
- . linear and quadratic approximations for the water height, together with quadratic approximation for the flow discharge, have given closely the same results ;
- . there exists some stability condition for the diffusion step : the nondimensional number  $(K.DT/DX^2)$  has to be more than about  $10^{-4}$  to avoid oscillations of the computed solution (probably because of the conflict arising between a nearly hyperbolic system to solve and boundary conditions related to the diffusion, i.e. prescribed velocity on the limits) ;
- . some kind of "overshoot" can appear in the advection step near the boundary when the flow gets out, due to a bad property of the quadratic interpolation on the flow discharge.

### 6.2. Dunkirk outer harbour

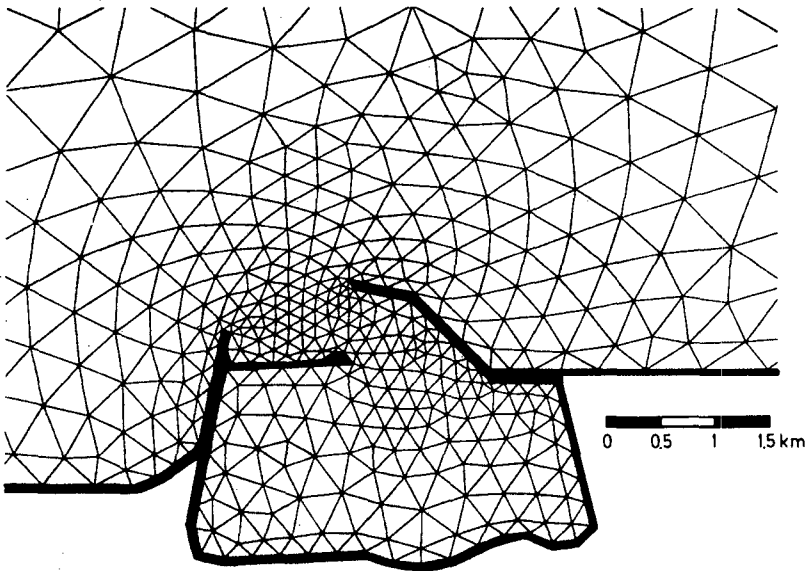
The second application, which is less schematic, concerns the computation of the tidal flow pattern in the vicinity of the new outer harbour of Dunkirk, located on the french coast of the North Sea.

This example has been chosen for two main reasons :

- . the shape of the domain and the complexity of the laying out of the limits give the typical case where a finite element method turns out to be specially suitable (good boundary representation and local refinement facilities) and provide a rather severe test of the model ;



a. Mesh of the whole area



b. Detail of the harbour

**Fig. 4 \_FINITE ELEMENTS MODEL OF DUNKIRK  
OUTER HARBOUR**

this case has been previously studied by means of a scale model and of a finite difference model ; so there exist references to which compare the results of the finite element model.

The finite element grid (fig.4) has been generated automatically by a program developed in our laboratory. As it can be noticed from this illustration, a special mesh refinement has been introduced near the limits, in order to obtain a better consideration of the boundary conditions (which is particularly useful for the land boundaries).

In this experiment a piecewise quadratic approximation has been used for each variable ; there are about nine hundred triangular elements and two thousand calculation nodes.

The characteristics of the computation are as follows :

- . tide range is about five meters ;
- . maximum velocity is about 1,5 m/s ;
- . tide and current are in phase (that is to say that the tide wave is here quite purely progressive) ;
- . eddy viscosity coefficient is equal to 5 m<sup>2</sup>/s ;
- . time step is sixty seconds and Courant number for propagation varies locally from 1 to 5.

Finally both components of the flow discharge are prescribed on the boundaries.

In fact two computations have been carried out successively in this case of Dunkirk : the first one under schematic conditions and the second one in a more realistic way.

#### 6.2.1. Schematic computation

In the first trial the flow discharge is assumed to be sinusoidal and parallel to the upper limit ; the bottom is flat and bed friction is not considered, just as in the example of Massachussets Bay.

Some instabilities appeared in the current field during the computation ; the problem turned out to come from the advection step, solved at first on the flow discharge Q :

$$\frac{\partial Q_i}{\partial t} + u^n \cdot \nabla Q_i = - Q_i \nabla \cdot u^n$$

The discontinuity of the term in the right hand side was found to be responsible for the instabilities. When using the formulation on velocity only, those instabilities actually disappeared.

Fig. 5 shows the evolution of the flow pattern in the vicinity of the harbour at the beginning of the flood current (slack occurs about three hours before high tide) : the flow deflection in front of the harbour and the formation of two eddies can be noticed :

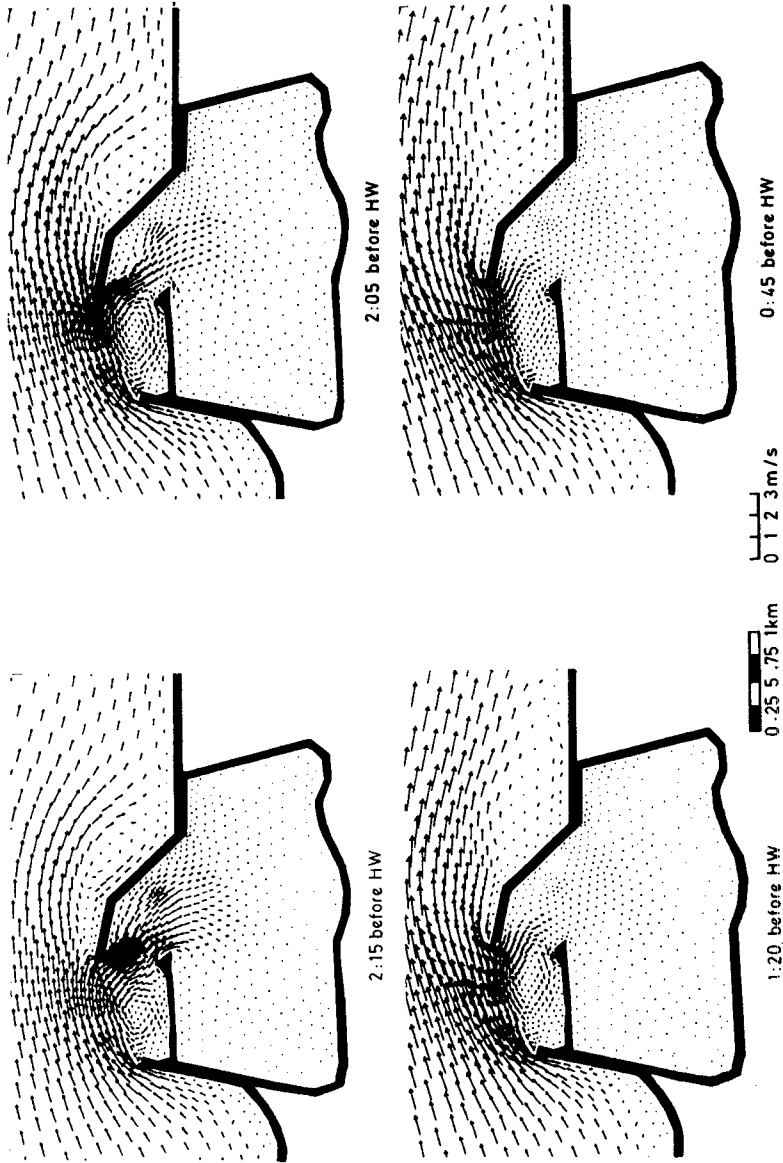


Fig. 5 - SCHEMATIC MODELISATION OF DUNKIRK OUTER HARBOUR  
Detail of the current fields

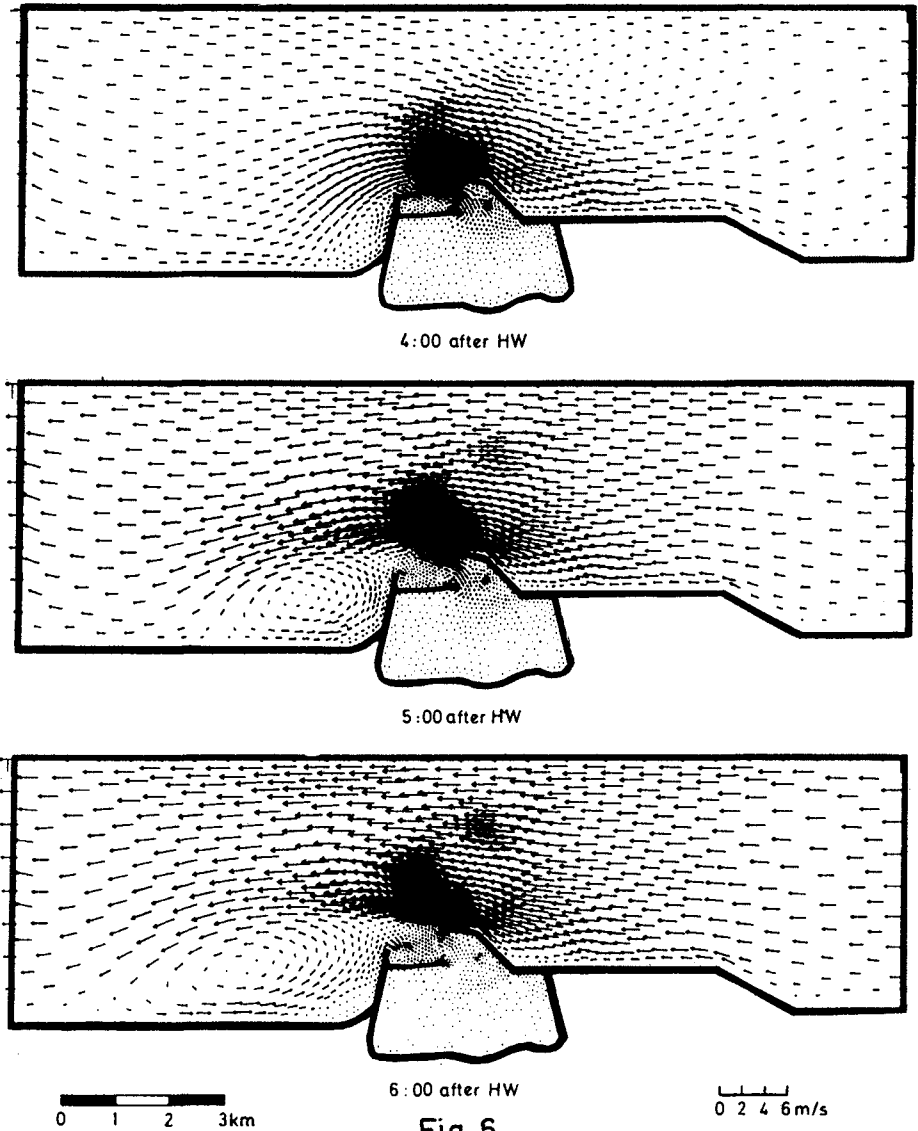


Fig. 6  
SCHEMATIC MODELISATION OF DUNKIRK OUTER HARBOUR  
COMPUTED CURRENTS IN THE WHOLE DOMAIN

- . The first one in the harbour entrance ; it becomes weaker and weaker as the harbour fills in.
- . The second eddy downstream the east jetty expands gradually eastwards and in fact it will fill at the end of the flood the whole eastern part of the domain because of the absence of bed friction and because the boundary conditions don't allow it to get out.

Fig. 6 points out in the whole domain the same phenomenon during the ebb : an eddy appears at the beginning of the ebb on the left of the west jetty and expands progressively till the end of the ebb.

Finally mass conservation was found to be as satisfying as for the first example ; here also the global error regarding the free surface elevation over one tide is less than 1 % of the tide range.

#### 6.2.2. Realistic computation

A second computation has been carried out after the insertion in the model of the bed friction and of the variability of the bed topography.

Fig. 7 exhibits the bathymetry in the vicinity of the harbour : the depths are quite variable, especially because of the navigation channel for oil tankers ; the steepness of the edges of the channel (about 1:10) is in fact a severe condition for the shallow water equations.

Boundary conditions are now deduced from the results of a previous computation made with a finite difference method on a larger domain.

The computation has been worked out during more than one tide, and the results have been compared to the data obtained by photographs of surface floats on the scale model, built about twelve years ago for the study of the new outer harbour.

Fig. 8 to 10 display this comparison during the most interesting period, from the beginning of the flood till high water.

On fig. 8, at the beginning of the flood, an eddy appears in a similar way on both models, just behind the end of the west jetty, while the harbour fills in ; half an hour later, both eddies have shifted and spread out likewise.

Afterwards (fig. 9) the eddy expands gradually till it covers the whole entrance in both models, with perhaps a slight difference in the shape. The flow deflection due to the harbour can be noticed farther than one kilometer away from the entrance in both cases.

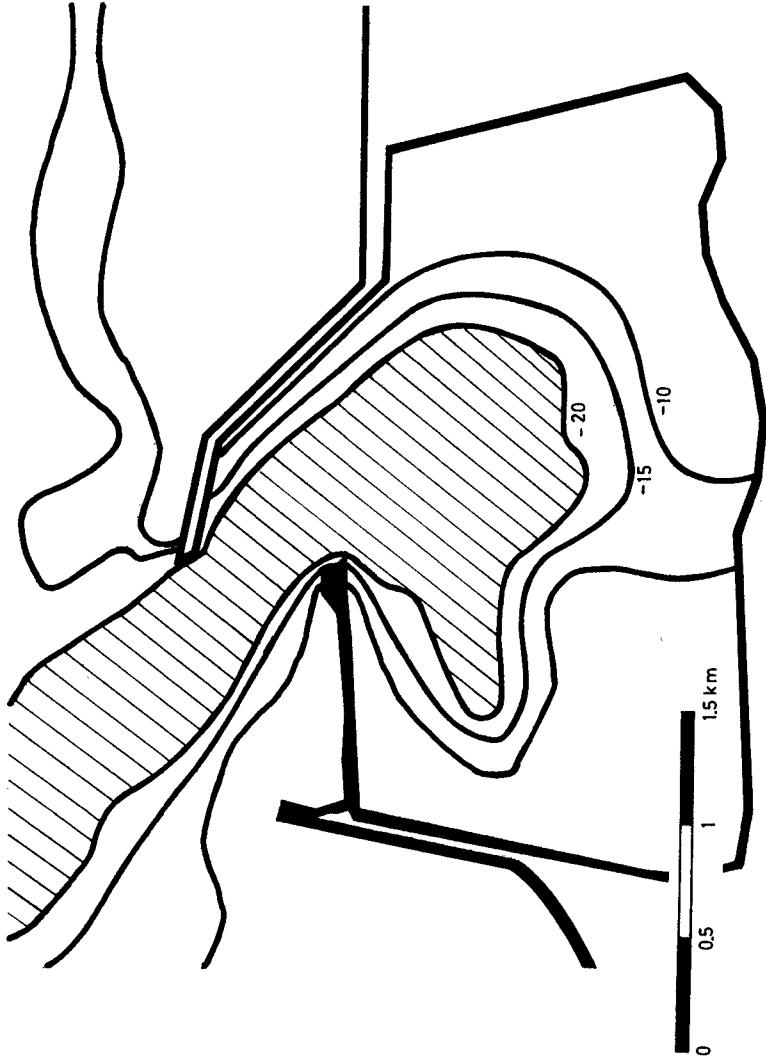


Fig.7 \_DUNKIRK OUTER HARBOUR REAL BED TOPOGRAPHY

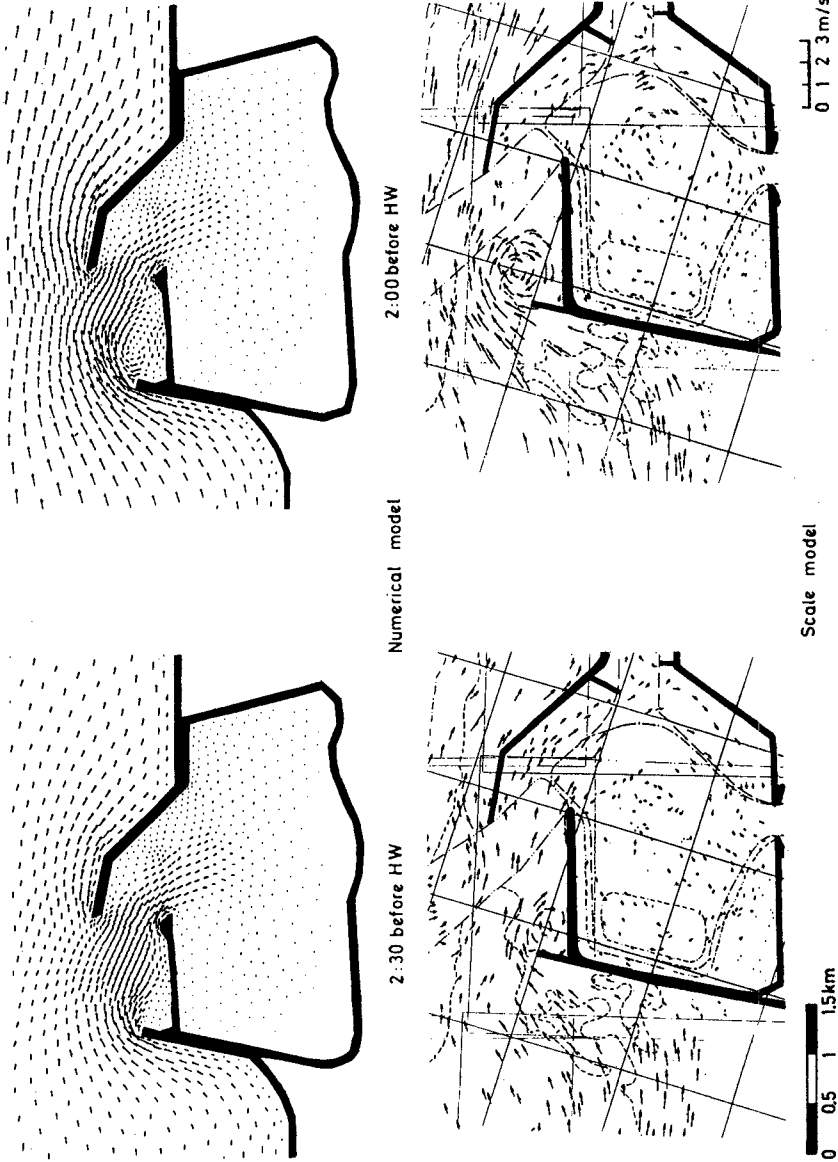


Fig. 8 - COMPARISON OF THE RESULTS OF NUMERICAL AND SCALE MODELS

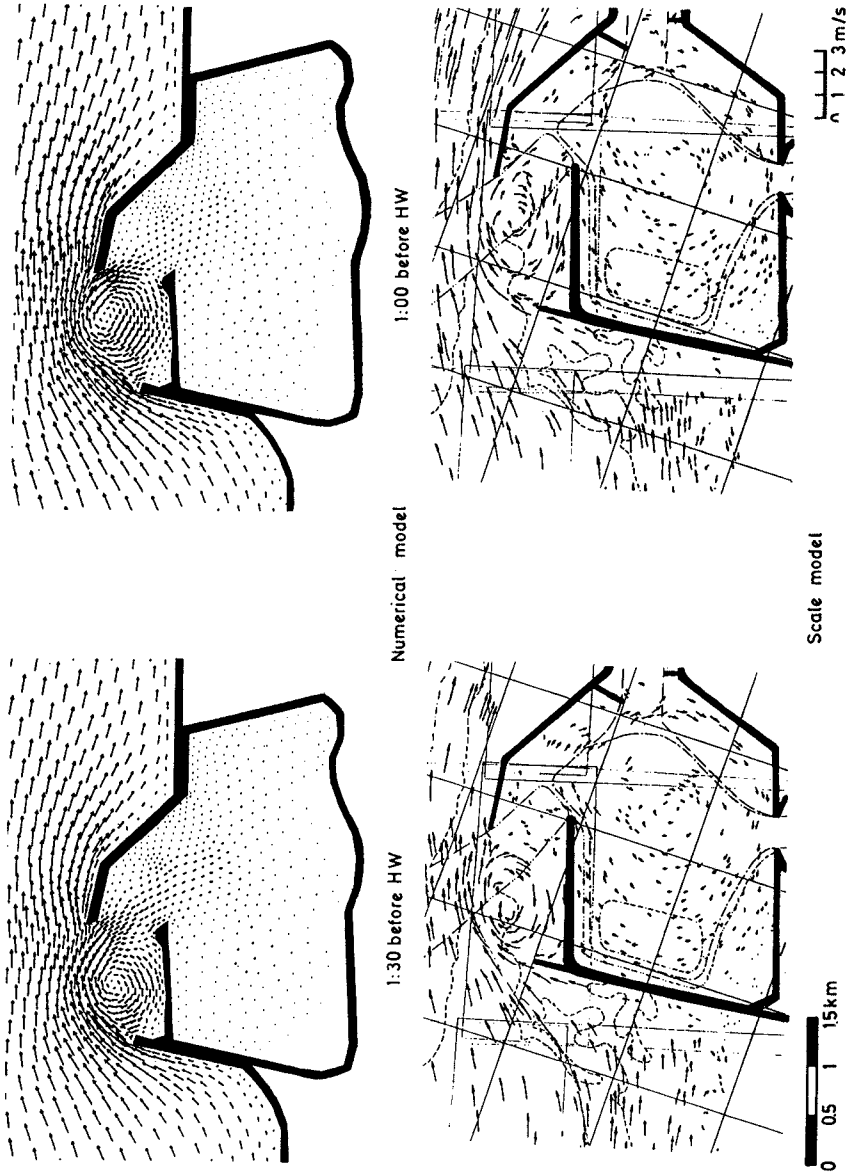


Fig. 9. COMPARISON OF THE RESULTS OF NUMERICAL AND SCALE MODELS

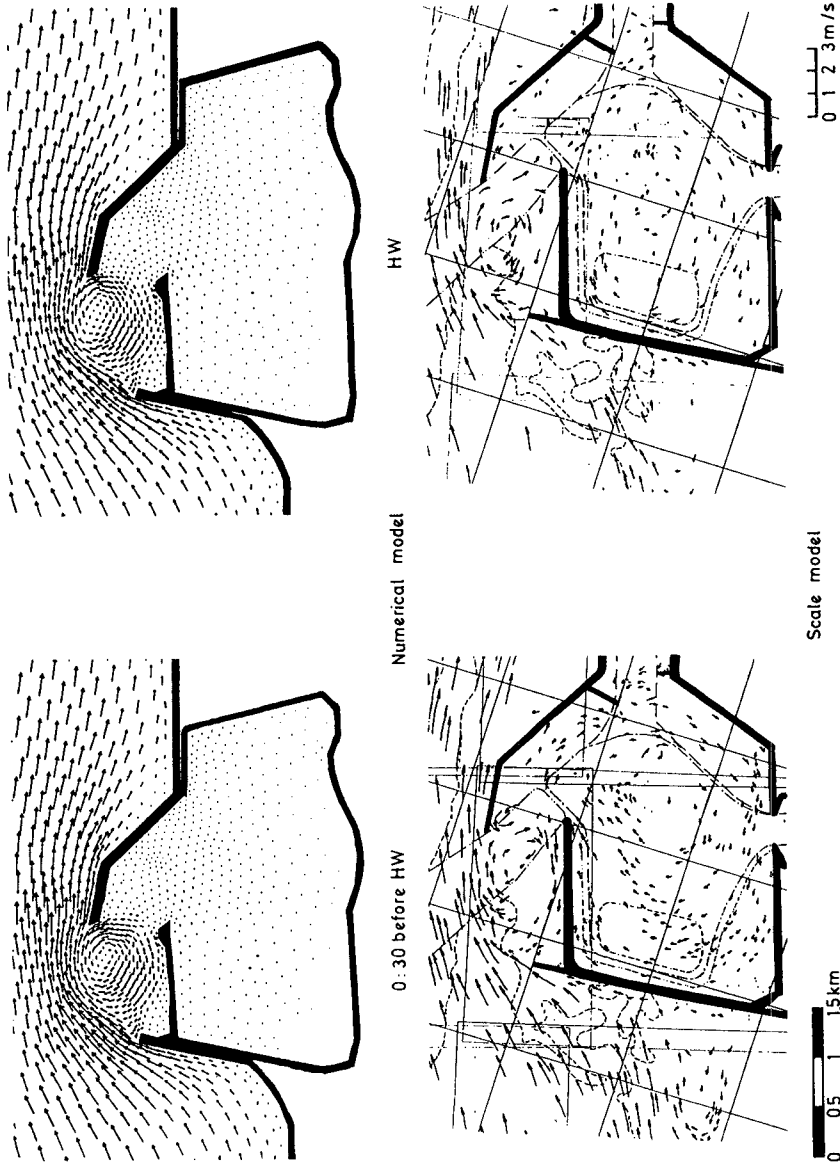


Fig.10 \_COMPARISON OF THE RESULTS OF NUMERICAL AND SCALE MODELS

From one hour before high water till high water (fig. 10) the eddy remains stable ; downstream the harbour, a slight flow separation can be noticed, but the computation does not develop a big eddy as in the case of the first computation (fig. 5).

The mass conservation is less accurately obtained than in the previous experiments ; the global level error over one tide is about 3 % of the tide range ; this seems to be due to the steepness of the sea bed near the breakwaters ; the problem can probably be overcome by taking a more severe threshold of convergence in the numerical resolution of the linear systems.

## 7. CONCLUSION

Compared to the classical finite difference method, which is now currently used to solve the shallow water equations, this finite element method presents many advantages, such as a better description of the boundaries and a greater flexibility of the grid ; on the other hand, the implementation of the model is rather longer and more complex, and involves a bigger consumption of processing time ; nevertheless, due to the special care given to reduce the size of the systems to be solved, the in-core memory requirements are quite reasonable. As an example computation over one tide (12 h 24 mn) using nearly 2 000 nodes of discretization and a time step of sixty seconds has required about 2 hours of CRAY 1 processing time and 1 000 K bytes of in-core memory.

Numerical experiments have clearly shown that even under rather severe conditions the model has a nice behaviour and exhibits a fair comparison with experimental data .

At present, improvements are in progress, with the implementation of an incident wave condition and the consideration of the influence of wind stress and atmospheric pressure field. The model will soon be used on a domain covering the whole English Channel up to the edge of the continental shelf (fig. 11), with two purposes :

- firstly to examine the impact of a possible tidal power plant on the tidal pattern in this area ;
- secondly to study the generation and propagation of storm surges in the English Channel.

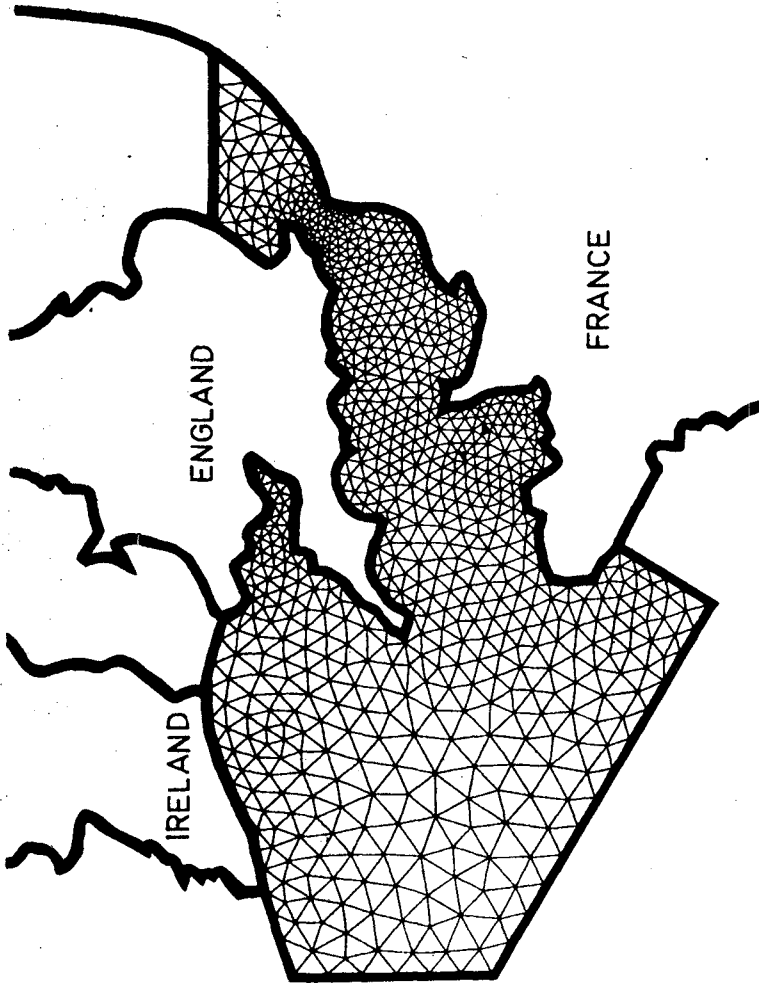


Fig.11 \_FINITE ELEMENTS MODEL OF THE ENGLISH CHANNEL

8. REFERENCES

1. J.P. Benqué, G. Labadie, B. Ibler

A finite element method for Navier-Stokes equations - First International Conference on numerical methods for non linear equations - Swansea, U.K., sept. 2nd - 5th 1980.

2. J.P. Benqué, J. Ronat

Quelques difficultés des modèles numériques en hydraulique - Fifth International Symposium on computing methods in applied sciences and engineering - INRIA, December 1981, Versailles, France.

3. M.O. Bristeau, R. Glowinski, J. Périaux, P. Perrier, O. Pironneau and G. Poirier

Application of optimal control and finite element methods to the calculation of transonic flows and incompressible viscous flows - Rapport de recherche 78-294, IRIA LABORIA, 78150 Le Chesnay, France.

5. G. Labadie, J.P. Benqué, B. Latteux

A finite element method for the shallow water equations - 2nd International Conference on numerical methods for laminar and turbulent flow, Venice, Italy, July 13-16 1981.

6. G. Labadie, B. Latteux

Résolution des équations de Saint-Venant par une méthode d'éléments finis - Rapports E.D.F. HE/41/82.15 et HE/42/82.34.